

# Mapping carbon accumulation potential from global natural forest regrowth

<https://doi.org/10.1038/s41586-020-2686-x>

Received: 15 March 2019

Accepted: 15 July 2020

Published online: 23 September 2020

 Check for updates

Susan C. Cook-Patton<sup>1,2</sup>✉, Sara M. Leavitt<sup>1</sup>, David Gibbs<sup>3</sup>, Nancy L. Harris<sup>3</sup>, Kristine Lister<sup>3</sup>, Kristina J. Anderson-Teixeira<sup>4,5</sup>, Russell D. Briggs<sup>6</sup>, Robin L. Chazdon<sup>3,7,8</sup>, Thomas W. Crowther<sup>9</sup>, Peter W. Ellis<sup>1</sup>, Heather P. Griscom<sup>10</sup>, Valentine Herrmann<sup>4</sup>, Karen D. Holl<sup>11</sup>, Richard A. Houghton<sup>12</sup>, Cecilia Larrosa<sup>13</sup>, Guy Lomax<sup>14</sup>, Richard Lucas<sup>15</sup>, Palle Madsen<sup>16</sup>, Yadvinder Malhi<sup>17</sup>, Alain Paquette<sup>18</sup>, John D. Parker<sup>2</sup>, Keryn Paul<sup>19</sup>, Devin Routh<sup>9</sup>, Stephen Roxburgh<sup>19</sup>, Sasan Saatchi<sup>20</sup>, Johan van den Hoogen<sup>9</sup>, Wayne S. Walker<sup>12</sup>, Charlotte E. Wheeler<sup>21</sup>, Stephen A. Wood<sup>22</sup>, Liang Xu<sup>20</sup> & Bronson W. Griscom<sup>23</sup>

To constrain global warming, we must strongly curtail greenhouse gas emissions and capture excess atmospheric carbon dioxide<sup>1,2</sup>. Regrowing natural forests is a prominent strategy for capturing additional carbon<sup>3</sup>, but accurate assessments of its potential are limited by uncertainty and variability in carbon accumulation rates<sup>2,3</sup>. To assess why and where rates differ, here we compile 13,112 georeferenced measurements of carbon accumulation. Climatic factors explain variation in rates better than land-use history, so we combine the field measurements with 66 environmental covariate layers to create a global, one-kilometre-resolution map of potential aboveground carbon accumulation rates for the first 30 years of natural forest regrowth. This map shows over 100-fold variation in rates across the globe, and indicates that default rates from the Intergovernmental Panel on Climate Change (IPCC)<sup>4,5</sup> may underestimate aboveground carbon accumulation rates by 32 per cent on average and do not capture eight-fold variation within ecozones. Conversely, we conclude that maximum climate mitigation potential from natural forest regrowth is 11 per cent lower than previously reported<sup>3</sup> owing to the use of overly high rates for the location of potential new forest. Although our data compilation includes more studies and sites than previous efforts, our results depend on data availability, which is concentrated in ten countries, and data quality, which varies across studies. However, the plots cover most of the environmental conditions across the areas for which we predicted carbon accumulation rates (except for northern Africa and northeast Asia). We therefore provide a robust and globally consistent tool for assessing natural forest regrowth as a climate mitigation strategy.

Restoring forest cover, defined here as the transition from less than 25% tree cover to more than 25% tree cover in areas where forests historically occurred, is a promising option for additional carbon capture<sup>3</sup> and has been prioritized in many national and international goals<sup>6,7</sup>. It is deployable, scalable and provides important biodiversity and ecosystem services<sup>8</sup>. Yet the magnitude and distribution of the climate mitigation opportunity available from restoring forest cover is poorly described, with large confidence intervals around estimates<sup>2,3</sup>. To evaluate the appropriateness of forest cover restoration for climate mitigation compared to the multitude of other potential climate mitigation

actions, countries, corporations, and multilateral entities need more accurate assessments of its potential<sup>9</sup>.

Mitigation potential from restoring forest cover is determined by the potential extent and location of restored forest ('area of opportunity') and the rate at which such forests remove atmospheric carbon (reported here in terms of megagrams of carbon per hectare per year, Mg C ha<sup>-1</sup> yr<sup>-1</sup>). Although there are multiple estimates of area of opportunity based on diverse and often heavily debated criteria (see for example refs. <sup>3,10–12</sup>), we lack spatially explicit and globally comprehensive estimates of carbon accumulation rates. This is especially true

<sup>1</sup>The Nature Conservancy, Arlington, VA, USA. <sup>2</sup>Smithsonian Environmental Research Center, Edgewater, MD, USA. <sup>3</sup>World Resources Institute, Washington, DC, USA. <sup>4</sup>Smithsonian Conservation Biology Institute, Front Royal, VA, USA. <sup>5</sup>Smithsonian Tropical Research Institute, Panama City, Panama. <sup>6</sup>State University of New York, College of Environmental Science and Forestry, Syracuse, NY, USA. <sup>7</sup>University of Connecticut, Storrs, CT, USA. <sup>8</sup>University of the Sunshine Coast, Sippy Downs, Queensland, Australia. <sup>9</sup>ETH Zurich, Zurich, Switzerland. <sup>10</sup>James Madison University, Harrisonburg, VA, USA. <sup>11</sup>University of California Santa Cruz, Santa Cruz, CA, USA. <sup>12</sup>Woods Hole Research Center, Falmouth, MA, USA. <sup>13</sup>Department of Zoology, University of Oxford, Oxford, UK. <sup>14</sup>Global Systems Institute, University of Exeter, Exeter, UK. <sup>15</sup>Aberystwyth University, Aberystwyth, UK. <sup>16</sup>InNovaSilva ApS, Vejle, Denmark. <sup>17</sup>Environmental Change Institute, School of Geography and the Environment, University of Oxford, Oxford, UK. <sup>18</sup>Centre for Forest Research, Université du Québec à Montréal, Montreal, Quebec, Canada. <sup>19</sup>CSIRO Land and Water, Canberra, Australian Capital Territory, Australia. <sup>20</sup>Jet Propulsion Laboratory, National Aeronautics and Space Administration, Pasadena, CA, USA. <sup>21</sup>School of Geosciences, University of Edinburgh, Edinburgh, UK. <sup>22</sup>Yale University, New Haven, CT, USA. <sup>23</sup>Conservation International, Arlington, VA, USA. ✉e-mail: susan.cook-patton@tnc.org

# Article

for natural forest regrowth, defined here as the recovery of forest cover on cleared lands through spontaneous regrowth after cessation of previous disturbance or land use. Many countries do not have nationally specific forest carbon accumulation rates and instead rely on default rates from the IPCC<sup>5,13</sup>. Although these rates were recently updated<sup>4,5</sup>, they nonetheless represent coarse estimates based on continent and ecozone, and do not account for finer-scale variation due to more local land-use history or environmental conditions. To reduce uncertainty and better predict variation in carbon accumulation rates, we have assembled a global dataset of carbon in naturally regrowing forests from the literature ('literature-derived data') and national inventory data. We used these data to assess how strongly climatic factors, soil characteristics and land-use history influenced variation in carbon accumulation rates and to produce a spatially explicit model of potential carbon accumulation across the globe. Throughout, we focused on the first thirty years of natural forest regrowth, because 2020 to 2050 represents a biophysically critical and policy-relevant window for reaching net zero emissions and limiting the most negative effects of global warming<sup>2,14</sup>.

We also focused on natural forest regrowth, although there are many ways to restore forest or tree cover (Extended Data Table 1) and these differ in utility depending on specific contexts. Although enthusiasm for tree planting is high, tree planting must be carefully planned to avoid negative outcomes, such as inappropriate species selection for a given site<sup>15</sup>, whereas natural forest regrowth may cost less and better promote the re-establishment of local biodiversity<sup>16,17</sup>. Reliance on natural forest regrowth, coupled with maintenance of natural disturbance regimes, also avoids perverse tree establishment in native grasslands<sup>18</sup>. Some reviews further suggest that naturally regrowing forests can recover as well as or better than actively restored forests<sup>19–22</sup>, although these reviews are probably biased towards sites more amenable for forest establishment, and natural forest regrowth can be limited by severe land degradation and distant seed sources<sup>23</sup>. Our comprehensive analysis across a range of starting conditions provides a robust baseline for natural forest regrowth and elucidates fundamental constraints and drivers of carbon accumulation rates. It also serves as a benchmark for alternative approaches to restoring forest cover, such as active tree planting, and provides a method of identifying areas with the greatest potential carbon accumulation per hectare.

## Potential drivers of accumulation rates

We used the literature-derived data to assess potential drivers of carbon accumulation rates. Biome type, as a proxy for climatic and environmental variation, significantly influenced carbon accumulation in total plant pools (that is, above- and belowground biomass combined). Total plant carbon accumulated more rapidly in warmer and wetter biomes than in cooler and drier ones ( $F$ -statistic with subscript degrees of freedom  $F_{5,2652.2} = 11.8, P < 0.0001$ ; Fig. 1). In contrast, soil carbon accumulation rates did not vary significantly across biomes ( $F_{6,126} = 1.0, P = 0.393$ ; Extended Data Fig. 1) or with soil texture ( $F_{9,128} = 0.2, P = 0.997$ ), underscoring the known challenges of generating default soil carbon accumulation rates<sup>5</sup>. In litter and coarse woody debris carbon pools, we did not observe measurable accumulation during the first 30 years of forest regrowth (Extended Data Fig. 2) despite differences among biomes in the absolute magnitude of these carbon pools (Extended Data Fig. 3). Indeed, carbon stocks in these pools often declined with time, presumably owing to decomposition of residual biomass from previous disturbance. We therefore did not further account for litter or coarse woody debris carbon since natural forest regrowth did not directly drive near-term carbon dynamics across our data.

The type of previous land use/disturbance significantly, but inconsistently, influenced carbon accumulation rates in both total plant and soil pools. The literature generally describes seven land-use/disturbance categories: pasture, long-term cropping, shifting cultivation, clear-cut

harvest, mining, fire and other natural disturbances (such as hurricane windthrow or landslide). In all forest biomes with the exception of the boreal biome, land-use/disturbance type significantly influenced total plant carbon accumulation (boreal:  $F_{1,21.1} < 0.1, P = 0.910$ ; temperate conifer:  $F_{4,32.1} = 31.3, P < 0.0001$ ; temperate broadleaf:  $F_{5,314.7} = 23.6, P < 0.0001$ ; tropical/subtropical dry:  $F_{1,539.8} = 13.7, P = 0.0002$ ; tropical/subtropical moist:  $F_{5,539.8} = 7.7, P < 0.0001$ ; and tropical/subtropical savanna:  $F_{2,48.0} = 3.2, P = 0.0495$ ). However, within a biome, rates were often similar across land-use/disturbance types (insets in Fig. 1). Moreover, across biomes, the specific effect of a given land-use/disturbance type often differed. For example, former cropland showed the highest rates of total plant carbon accumulation in the temperate broadleaf biome, but only intermediate rates in the tropical/subtropical moist biome. For soil, previous land use/disturbance data were limited to temperate broadleaf and tropical/subtropical moist forests. Only temperate broadleaf forests showed a significant effect; specifically, that disturbance caused by cropping or timber harvest led to faster soil accumulation than disturbance by pasture ( $F_{2,46} = 7.5, P = 0.001$ ). Overall, these results suggest that land-use/disturbance type cannot be used to predict carbon accumulation rates in naturally regrowing forests at global scales owing to inconsistent effects across biomes for total plant carbon and limited data for soil.

Finally, disturbance intensity influenced carbon accumulation in plant biomass ( $F_{2,992.3} = 13.7, P < 0.0001$ ) but not soil ( $F_{2,78} = 1.4, P = 0.237$ ). The literature-derived data included sites that experienced a range of disturbance intensities, from relatively mild (for example, most natural disturbance) to very intense (for example, long-term tillage for agriculture), so we categorized sites according to low, medium or high disturbance intensity (see Supplementary Table S1). In general, total plant carbon accumulation rates were greater after the highest intensity of disturbance compared to the lowest intensity of disturbance (Extended Data Fig. 4), but this pattern was not consistent across biomes. Instead, within biomes, the highest carbon accumulation rates occurred in the category with the lowest starting biomass, regardless of disturbance intensity (Extended Data Table 2), reflecting standard sigmoidal growth curves.

## Mapping carbon accumulation rates

Given the significant biome effects and the limited predictive power of land-use/disturbance history, we used 66 global environmental covariate layers, primarily related to climate (see Supplementary Table S2), to develop a global map of potential aboveground carbon accumulation rates at a 1-km scale. We modelled only aboveground carbon accumulation, because the aboveground data represented the largest fraction of our literature-derived data ( $N = 2,118$ ), showed strong and well explained variation across the globe, and avoided propagating uncertainty from root-to-shoot ratios. Focusing on aboveground carbon also allowed us to improve our geographic and environmental representation with available aboveground carbon data from national forest inventories in Australia, Sweden and the USA ( $N = 10,994$ ). However, to increase the utility of these maps for conservation and policy planning, we estimated belowground carbon post hoc using IPCC default root-to-shoot ratios<sup>5</sup> (see 'Data availability' section).

We used an ensemble machine-learning model to develop a predictive map of aboveground carbon accumulation rates in naturally regenerating forests over the next 30 years (Fig. 2a). Rates ranged from  $0.058 \text{ Mg C ha}^{-1} \text{ yr}^{-1}$  to  $6 \text{ Mg C ha}^{-1} \text{ yr}^{-1}$ . The best ensemble model included all 66 covariate layers and predicted the test data reasonably well (root-mean-square error RMSE =  $0.80 \text{ Mg C ha}^{-1} \text{ yr}^{-1}, R^2 = 0.45$ ). Our model required limited extrapolation to environmental conditions not included in the training plots, with covariate values at the field sites spanning most of the range of covariate values across the entire prediction area (Extended Data Fig. 5). The standard deviation across the ensemble model was  $\pm 13\%$  of the predicted value, on average, but

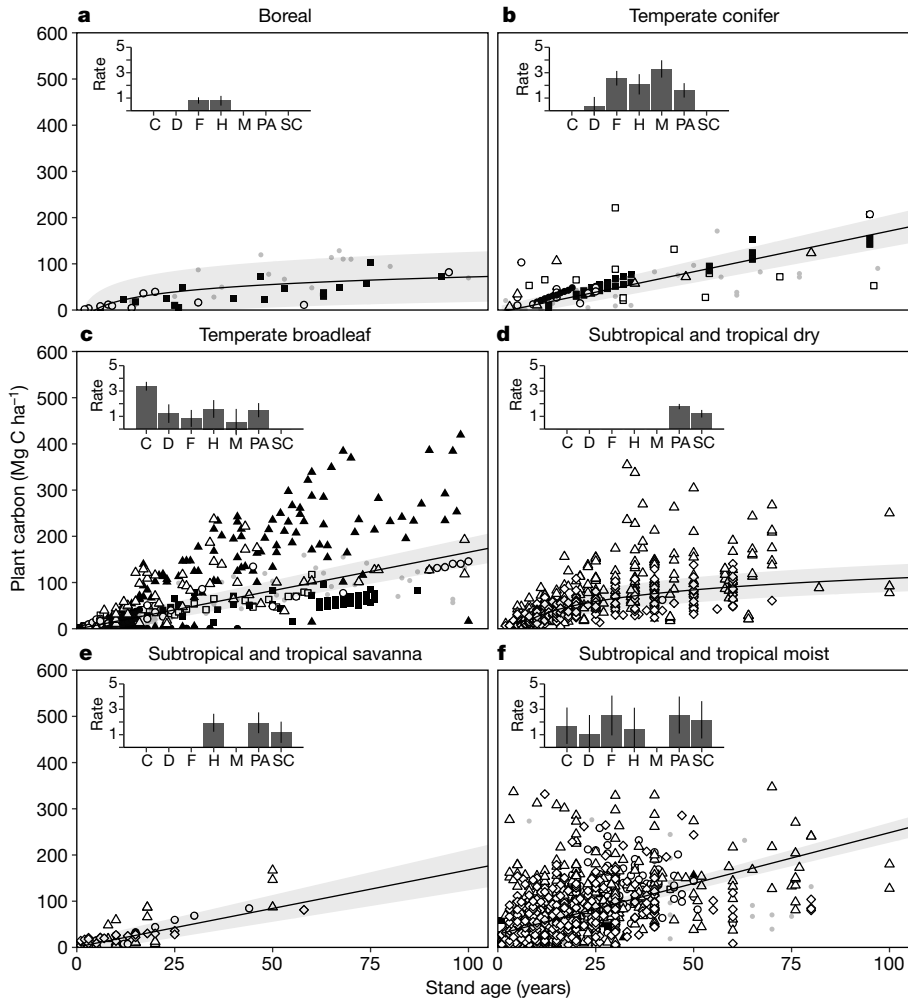


**Fig. 1 | Variation in carbon accumulation among biomes and previous land use/disturbance.** Scatterplots show total plant carbon through time from the literature-derived data ( $\text{Mg C ha}^{-1} \pm 95\%$  confidence interval) regardless of disturbance. Insets show average carbon accumulation rates as a function of previous land use/disturbance from the literature-derived data ( $\text{Mg C ha}^{-1} \text{yr}^{-1} \pm 95\%$  confidence interval). Studies usually provided information on seven disturbance/land-use types: fire (F, filled squares), other natural disturbance (D, open squares, such as hurricane windthrow), clear-cut harvest of land in forest use (H, open circles), shifting cultivation (SC, open diamonds), pasture (PA, open triangles), permanent cropland (C, closed triangles), and mining (M, closed circles). Small grey points indicate no known disturbance type. Biomes include: **a**, boreal ( $N_{\text{scatterplot}} = 45$ ;  $N_{\text{inset}} = 18$  (F), 11 (H)); **b**, temperate conifer ( $N_{\text{scatterplot}} = 104$ ;  $N_{\text{inset}} = 12$  (D), 39 (F), 13 (H), 10 (M), 7 (PA)); **c**, temperate broadleaf ( $N_{\text{scatterplot}} = 418$ ;  $N_{\text{inset}} = 113$  (C), 32 (D), 47 (F), 50 (H), 69 (M), 51 (PA)); **d**, subtropical/tropical dry ( $N_{\text{scatterplot}} = 552$ ;  $N_{\text{inset}} = 233$  (PA), 316 (SC)); **e**, subtropical/tropical savanna ( $N_{\text{scatterplot}} = 57$ ;  $N_{\text{inset}} = 13$  (H), 21 (PA), 23 (SC)) and **f**, subtropical/tropical moist ( $N_{\text{scatterplot}} = 1614$ ;  $N_{\text{inset}} = 32$  (C), 4 (D), 68 (F), 139 (H), 648 (PA), 628 (SC)). Savanna results apply only to the portions of these grassland-forest matrices with forest cover exceeding 25%.

areas of substantial uncertainty remain. We observed the highest uncertainty in northern Africa and northeast Asia, and lowest uncertainty in the tropics (Fig. 2b).

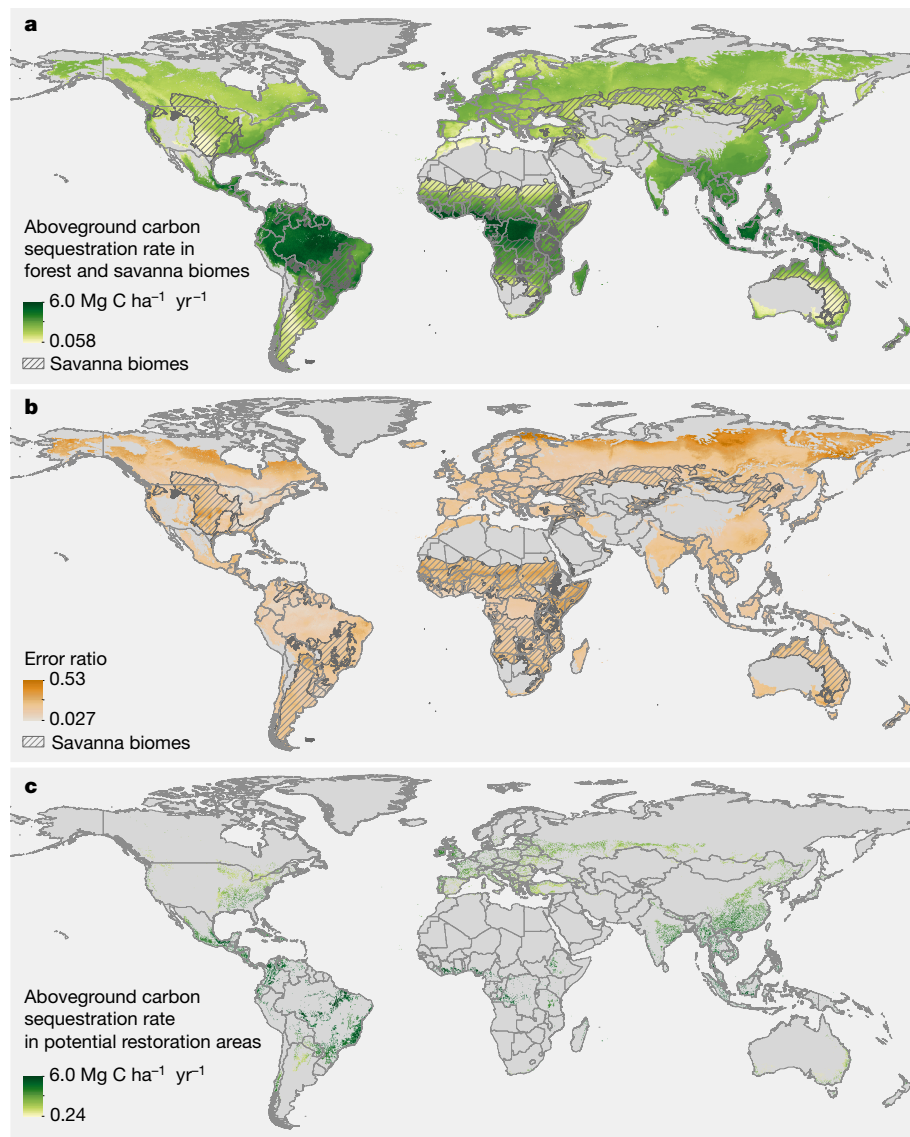
When we examined average carbon accumulation rates using the same spatial boundaries underlying the 2019 IPCC defaults (that is, United Nations Food and Agriculture Organization (FAO) ecozones crossed by continent)<sup>5</sup>, we found that our predicted rates were 32% higher on average than IPCC defaults for young forests (Fig. 3). However, this differed within and across biomes. Notably, our predicted rates were consistently higher (53% on average) in the tropical biomes compared to 2019 IPCC defaults, even though some of our input data were used to update these IPCC rates<sup>4</sup>. Our predicted rates are also on the high end of the range provided by the IPCC for the boreal biome, though incorporating albedo effects will limit the climate mitigation potential of natural forest regrowth in these locations<sup>24</sup>.

Our map of potential carbon accumulation rates also demonstrated the value of improved spatial resolution, with over eight-fold variation within an average FAO ecozone and continent combination (that is, the difference between the maximum and minimum predicted value relative to the minimum). Variation within countries was also substantial, with an average of 1.7-fold difference in rates within a country (see Supplementary Information) and notable differences in rates at small spatial scales (see Colombia as an example, in Extended Data Fig. 6).

## Climate mitigation potential of regrowth

Our map of potential near-term carbon accumulation rates also allowed us to refine estimates of global mitigation potential from natural forest

regrowth. To do so, we combined our rate map with two scenarios of forest expansion based on recently published estimates. Although there are multiple and diverse estimates of area of opportunity<sup>3,10–12</sup>, we chose two that represent a policy-relevant scenario and a maximum biophysical potential. The first ‘national commitments’ scenario combines country-level commitments to the Bonn Challenge and nationally determined contributions to the Paris Agreement (349 Mha; based on ref.<sup>12</sup>). The second ‘maximum’ scenario is a spatially resolved estimate of maximum biophysical area (678 Mha) that excludes grassland biomes to avoid negative biodiversity consequences, the boreal biome owing to potentially adverse warming effects from changes in albedo, current croplands to safeguard human needs for food, and rural and urban population centres<sup>3</sup> (Fig. 2c). Using our maps of potential above-ground carbon accumulation, we estimate that 30 years of natural forest regrowth across 349 Mha and 678 Mha could capture 1.08 and 1.60 petagrams of carbon per year ( $\text{Pg C yr}^{-1}$ ) in aboveground biomass, respectively, and a further 0.37 and 0.54  $\text{Pg C yr}^{-1}$  in belowground biomass, respectively. Carbon accumulation in soil may be negligible or negative (Extended Data Fig. 1). However, if we use the global average from our literature-derived data ( $0.42 \text{ Mg C ha}^{-1} \text{yr}^{-1}$ ) for the shallower 0–30 cm profile where additional soil accumulation is expected to occur<sup>25</sup>, then these estimates rise to a total of 1.60 and 2.43  $\text{Pg C yr}^{-1}$ , respectively. Under the national commitments scenario<sup>12</sup>, the top ten countries held 69% of the global mitigation potential, whereas under the maximum scenario<sup>3</sup>, the top ten countries held 61% of the potential (see Supplementary Dataset 1). However, these countries differed between scenarios, and in general mitigation potential depended heavily on area of opportunity. These two scenarios are illustrative and

**Fig. 2 | Mapping carbon accumulation potential.**

**a**, Predicted aboveground carbon accumulation rates ( $\text{Mg C ha}^{-1} \text{yr}^{-1}$ ) in naturally regrowing forests in forest (solid colours) and savanna biomes (hatched colours). We denote savanna biomes differently to note that many of these areas are not appropriate for forests and that restoration of forest cover should proceed with particular caution in these biomes. We note that the map only predicts accumulation rates if natural forest 30 years old or less were growing there; it does not exclude currently forested areas or non-forestable parts of these biomes. **b**, The ratio of model uncertainty relative to best-fit model value per 1-km pixel. Higher ratios denote greater variation across random forest decision trees. **c**, Modelled accumulation rates restricted to the area of opportunity in Griscom et al.<sup>3</sup> to demonstrate where these rates might apply. D.G. created the maps in Fig. 2 and Extended Data Figs. 5–7 using ArcMap version 10.6.

alternative scenarios would provide different results. Regardless, the mitigation potential of any scenario can easily be estimated using the global map presented here.

## Evaluation of our results

Enthusiasm is high for natural forest regrowth as a climate mitigation strategy, given its potential to capture carbon while also providing additional benefits, such as habitat for biodiversity<sup>8</sup>, which is needed to ameliorate the equally urgent biodiversity crisis<sup>26</sup>. Here, we provide a consistent method for quantifying potential carbon accumulation in naturally regrowing forests over the next 30 years, at global and local scales. We find that current IPCC default rates are on average 32% lower than our predicted rates and most notably 53% lower in the tropics, suggesting that tropical countries using IPCC default rates may underestimate the mitigation potential of natural forest regrowth. Moreover, the default IPCC rates do not capture eight-fold variation within eco-zones. Requena Suarez et al.<sup>4</sup> provide a thorough description of the methods used to generate the IPCC tropical and subtropical defaults. Compared to those methods, we had more extensive data coverage, with field measurements in 32 rather than 12 of the subtropical/tropical ecozone by continent combinations. We used individual field plots and assumed linear growth rates, rather than chronosequences or

permanent plots and log-linear growth rates, to generate each rate estimate and have ten times more rate estimates per ecozone by continent combination. Further, we combined the field measurements with 66 environmental covariates, allowing us to predict potential carbon accumulation rates at much finer spatial resolution.

The improved spatial resolution of our study also allows us to better match area of opportunity with potential carbon accumulation rates and refine previous estimates of climate mitigation potential. We find that the maximum biophysical potential for natural forest regrowth to mitigate climate change is  $2.43 \text{ Pg C yr}^{-1}$ , which is almost 11% lower than previously reported<sup>3</sup> owing to the overestimation of rates. The area-weighted average carbon accumulation rate in Griscom et al.<sup>3</sup> was  $3.58 \text{ Mg C ha}^{-1} \text{yr}^{-1}$  (derived from Bonner et al.<sup>27</sup>) compared to the  $3.16 \text{ Mg C ha}^{-1} \text{yr}^{-1}$  estimated here. Nevertheless, even with our more conservative rate estimates<sup>3</sup>, regrowth of natural forest in the absence of cost constraints remains the single largest natural climate solution.

Achieving  $2.43 \text{ Pg C yr}^{-1}$  under our maximum biophysical scenario is challenging and would require dietary shifts towards a plant-based diet, which could release large areas of current grazing lands back to forest, as well as croplands that are used to produce fodder for livestock<sup>28,29</sup>. Even  $1.60 \text{ Pg C yr}^{-1}$  under the more policy-relevant national commitments scenario will be difficult to achieve, with some countries committing to the restoration of more forest area than is available<sup>11</sup> and

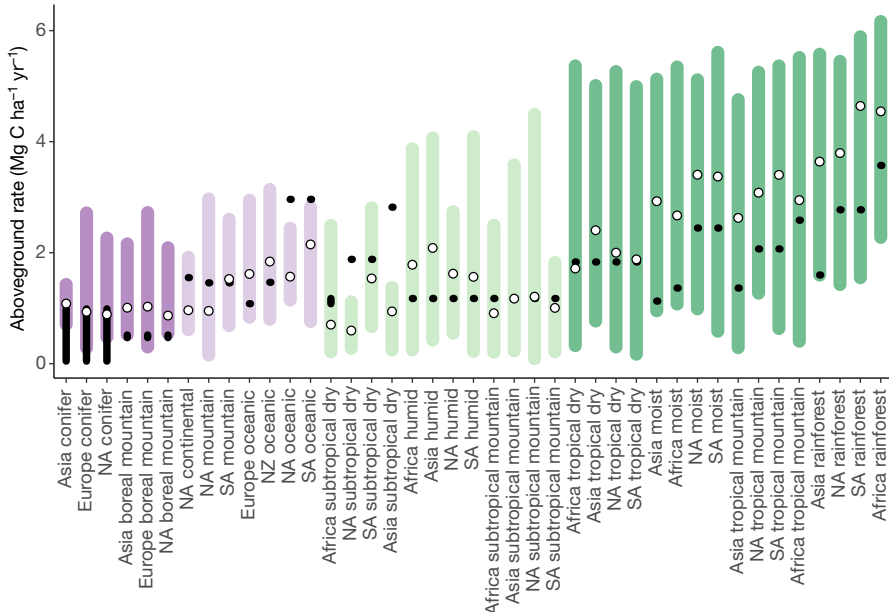


**Fig. 3 | Predicted rates compared to IPCC defaults.** Average predicted rate of carbon accumulation per ecozone (open circles) compared to 2019 IPCC defaults, which are given as a single number (filled circle) or a range (thick black bars). Coloured bars indicate the range between the minimum and maximum modelled rate per ecozone and continent (boreal, dark purple; temperate, light

purple; subtropical, light green; and tropical, dark green). Ecozone and continental forest types are listed below the x axis (NA, North America; NZ, New Zealand; SA, South America). We assume linear growth rate during the first 30 years and thus can compare our rates to the IPCC rates for young forests less than 20 years old.

relying on approaches other than natural forest regrowth to restore forests<sup>12</sup>. These challenges do not undermine the utility of our map, however, which can be used to estimate mitigation potential for any area of opportunity ranging from project-level to alternative global estimates, such as the one provided in Bastin et al.<sup>11</sup>.

The urgency of the growing climate crisis means that the global community needs to simultaneously deploy multiple climate mitigation strategies to constrain global warming<sup>12</sup>. This includes strong reductions in emissions, since natural climate solutions, including the regrowth of natural forests, are not a substitute for reducing fossil fuel emissions<sup>30</sup>, but rather an essential complement, especially while carbon capture technologies remain expensive and under development<sup>31</sup>. Regrowing natural forest is also not a substitute for protecting existing forests, which store enormous pools of carbon<sup>32</sup>. In general, there is no ‘panacea’ approach to climate mitigation and most, if not all, options (for example, transformations in the energy sector, carbon taxes) will require enormous political will and financial resources to realize. Natural forest regrowth may impose land-use trade-offs<sup>3,10</sup>, but our results can help local decisionmakers optimize areas of opportunity for natural forest regrowth by pinpointing areas of high potential carbon accumulation to consider alongside other important feasibility criteria, such as costs, livelihoods, and social suitability<sup>10</sup>.

Our analyses of carbon accumulation rates also complement other global mapping efforts that focus on long-term carbon storage in mature forests<sup>11,33,34</sup> or to 2100<sup>12</sup>, serving as a counterpoint to assumptions around the time frame and carbon accumulation rates needed to achieve these long-term carbon stores. For example, achieving the maximum carbon storage in Bastin et al.<sup>11</sup> (205 PgC across 900 Mha) within 100 years would require 2.28 Mg C ha<sup>-1</sup> yr<sup>-1</sup>. Although that analysis identified a very large area of opportunity, the rate estimate is moderate given our range of potential carbon accumulation rates. Further, although long-term storage is important, the next thirty years represent an important and policy-relevant window for limiting global warming<sup>2,14</sup> and our rate estimates facilitate comparisons of natural forest regrowth with other near-term climate mitigation actions.

There are several sources of uncertainty in our analysis. The first results from limited field site coverage, and variation in data quality and methodology. Although our data compilation far exceeds previous efforts with an initial consideration of 11,360 publications, confidence in our results necessarily depends on data availability, which varies considerably across studies and locations (Extended Data Fig. 7). The dataset employed here spanned 43 countries, but 96% of the data were derived from only ten countries (the USA, Sweden, Mexico, Brazil, Costa Rica, Colombia, China, Indonesia, Bolivia and Panama, in descending order of amount of data). Data may be limited because researchers have not collected sufficient amounts, the data are not publicly available (as for many national forest inventories), and/or some forest types are still fairly intact with limited opportunity to quantify regrowth. Despite the patchy plot data, we found that plots covered most of the environmental conditions across the prediction area, with the main exceptions being the Sahel and northeast Asia (Extended Data Fig. 5).

Increased data collection, ideally in a coordinated fashion to facilitate greater comparability across sites and using repeated plot measurements to improve robustness, would ameliorate some of these issues. To facilitate coordination and enable updates to our analyses as new data become available, we deliberately merged our efforts with the global Forest Carbon Database (ForC) to support the further development of a single, robust, and transparent repository for forest carbon data<sup>35</sup>. Future data collection should not only prioritize aboveground carbon data in more poorly sampled geographies, but also soil carbon data. Although our review encompasses and expands upon all existing reviews of soil carbon accumulation (see Methods), the available data did not substantially elucidate how soil carbon changes with natural forest regrowth. Our global default of 0.42 Mg C ha<sup>-1</sup> yr<sup>-1</sup> for soil carbon accumulation is similar to that observed by others (for example, refs. <sup>25,36</sup>), but further research is clearly merited.

Another source of uncertainty stems from using historical forest growth to predict future carbon accumulation rates. As global warming ramps up, rates in a given location may increase or decrease depending on factors such as disturbance frequency, carbon dioxide fertilization, or increased respiration due to higher temperatures<sup>11,37</sup>. Moreover,

there are other known factors that influence natural forest regrowth that we did not capture in our analysis. For example, residual vegetation can accelerate forest regrowth by providing roosting sites for seed-dispersers<sup>38</sup> or shade for late-successional species<sup>39</sup>. Others have observed an increased likelihood of regrowth near rivers or existing forest fragments, far from roads or on steep (less-accessible) slopes, and in areas protected from browsing<sup>40–43</sup>. Our global map provides a good starting point, but project-level planning will require detailed site assessments, as well as additional research to refine how local factors and future climate will affect carbon accumulation rates in a given location.

Further work is also needed to characterize how other approaches to restoring forest cover affect carbon accumulation rates and storage. We focused on natural forest regrowth, where natural processes rather than management actions predominantly drive carbon accumulation. However, the permanence of natural forest regrowth (and the carbon stored therein) cannot be assumed<sup>44</sup>, especially if secondary forests are less valued than plantation forests. Rates from naturally regrowing forests also do not capture how silvicultural practices can enhance tree establishment and carbon accumulation<sup>45</sup> or how harvested wood products from sustainably managed forests can be substituted for more energy-intensive products and provide carbon storage in long-lived wood products<sup>46</sup>. Additional work is needed to characterize climate mitigation potential of alternative management schemes, but we now provide a robust baseline from which to characterize any additional benefit of assisted regeneration and active planting and management<sup>19–23</sup>.

As countries, corporations, and multilateral entities develop plans to deploy natural forest regrowth as a climate mitigation strategy, our global, 1-km-resolution map of potential aboveground carbon accumulation rates should provide essential information for targeting activities towards areas with the highest potential carbon accumulation, estimating the potential carbon return on investment, and further refining how forests influence terrestrial carbon cycles at local, national and global scales. It will allow governments that have nationally determined contributions related to natural forest regrowth to estimate potential carbon accumulation quickly and prioritize more detailed assessments. We thus enable more robust comparisons of natural forest regrowth to other climate mitigation options and confirm that regrowing natural forests can strongly contribute to stabilizing global warming.

## Online content

Any methods, additional references, Nature Research reporting summaries, source data, extended data, supplementary information, acknowledgements, peer review information; details of author contributions and competing interests; and statements of data and code availability are available at <https://doi.org/10.1038/s41586-020-2686-x>.

- Rogelj, J. et al. Paris Agreement climate proposals need boost to keep warming well below 2°C. *Nat. Clim. Chang.* **534**, 631–639 (2016).
- Masson-Delmotte, V. et al. (eds) *Global Warming of 1.5 °C. An IPCC Special Report on the Impacts of Global Warming of 1.5 °C Above Pre-industrial Levels and Related Global Greenhouse Gas Emission Pathways, in the Context of Strengthening the Global Response to the Threat of Climate Change, Sustainable Development, and Efforts to Eradicate Poverty* (IPCC, 2018).
- Griscom, B. W. et al. Natural climate solutions. *Proc. Natl Acad. Sci. USA* **114**, 11645–11650 (2017).
- Requena Suarez, D. et al. Estimating aboveground net biomass change for tropical and subtropical forests: refinement of IPCC default rates using forest plot data. *Glob. Chang. Biol.* **25**, 3609–3624 (2019).
- Dong, H., MacDonald, J. D., Ogle, S. M., Sanz Sanchez, M. J. & Rocha, M. T. (eds) 2019 Refinement to the 2006 IPCC Guidelines for National Greenhouse Gas Inventories. Volume 4: Agriculture, Forestry and Other Land Use (IPCC, 2019).
- Grassi, G. et al. The key role of forests in meeting climate targets requires science for credible mitigation. *Nat. Clim. Chang.* **7**, 220–226 (2017).
- International Union for Conservation of Nature infoFLR <https://infoflr.org/> (IUCN, accessed 20 June 2018).
- Lamb, D., Erskine, P. D. & Parrotta, J. A. Restoration of degraded tropical forest landscapes. *Science* **310**, 1628–1632 (2005).
- Seddon, N. et al. Understanding the value and limits of nature-based solutions to climate change and other global challenges. *Phil. Trans. R. Soc. Lond. B* **375**, 20190120 (2020).
- Brancalion, P. H. S. et al. Global restoration opportunities in tropical rainforest landscapes. *Sci. Adv.* **5**, eaav3223 (2019).
- Bastin, J.-F. et al. The global tree restoration potential. *Science* **365**, 76–79 (2019).
- Lewis, S., Wheeler, C. E., Mitchard, E. T. A. & Koch, A. Regenerate natural forests to store carbon. *Nature* **568**, 25–28 (2019).
- Romijn, E. et al. Assessing change in national forest monitoring capacities of 99 tropical countries. *For. Ecol. Manage.* **352**, 109–123 (2015).
- United Nations Adoption of the Paris Agreement [https://unfccc.int/files/essential\\_background/convention/application/pdf/english\\_paris\\_agreement.pdf](https://unfccc.int/files/essential_background/convention/application/pdf/english_paris_agreement.pdf) (UN, 2015).
- Holl, K. D. & Brancalion, P. S. Tree planting is not a simple solution. *Science* **368**, 580–582 (2020).
- Gilroy, J. J. et al. Cheap carbon and biodiversity co-benefits from forest regeneration in a hotspot of endemism. *Nat. Clim. Chang.* **4**, 503–507 (2014).
- Chazdon, R. L. Landscape restoration, natural regeneration, and the forests of the future. *Ann. Missouri Botan. Gardens* **102**, 251–257 (2017).
- Veldman, J. W. et al. Tyranny of trees in grassy biomes. *Science* **347**, 484–485 (2014).
- Meli, P. et al. A global review of past land use, climate, and active vs. passive restoration effects on forest recovery. *PLoS One* **12**, e0171368 (2017).
- Crouzelles, R. et al. Ecological restoration success is higher for natural regeneration than for active restoration in tropical forests. *Sci. Adv.* **3**, e1701345 (2017).
- Jones, H. P. et al. Restoration and repair of Earth's damaged ecosystems. *Proc. R. Soc. Lond. B* **285**, 20172577 (2018).
- Shimamoto, C. Y., Padial, A. A., Da Rosa, C. M. & Marques, M. C. M. Restoration of ecosystem services in tropical forests: a global meta-analysis. *PLoS One* **13**, e0208523 (2018).
- Reid, J. L., Fagan, M. E. & Zahawi, R. A. Positive site selection bias in meta-analyses comparing natural regeneration to active forest restoration. *Sci. Adv.* **4**, eaas9143 (2018).
- Betts, R. A. Climate science: afforestation cools more or less. *Nat. Geosci.* **4**, 504–505 (2011).
- Nave, L. E. et al. Reforestation can sequester two petagrams of carbon in US topsoils in a century. *Proc. Natl Acad. Sci. USA* **115**, 2776–2781 (2018).
- Brondizio, E. S., Settele, J., Diaz, S. & Ngo, H. T. (eds) *The Global Assessment Report on Biodiversity and Ecosystem Services* <https://ipbes.net/global-assessment> (IPBES, 2019).
- Bonner, M. T. L., Schmidt, S. & Shoo, L. P. A meta-analytical global comparison of aboveground biomass accumulation between tropical secondary forests and monoculture plantations. *For. Ecol. Manage.* **291**, 73–86 (2013).
- Tuomisto, H. L., Ellis, M. J. & Hastrup, P. Environmental impacts of cultured meat production. *Environ. Sci. Technol.* **45**, 6117–6123 (2014).
- Arneth, A. et al. *Climate Change and Land: An IPCC Special Report on Climate Change, Desertification, Land Degradation, Sustainable Land Management, Food Security, And Greenhouse Gas Fluxes In Terrestrial Ecosystems* <https://www.ipcc.ch/srccl/> (IPCC, 2019).
- Griscom, B. W. et al. We need both natural and energy solutions to stabilize our climate. *Glob. Change Biol.* **25**, 1889–1890 (2019).
- Field, C. B. & Mach, K. J. Rightsizing carbon dioxide removal. *Science* **356**, 706–707 (2017).
- Goldstein, A. et al. Protecting irrecoverable carbon in Earth's ecosystems. *Nat. Clim. Chang.* **10**, 287–295 (2020).
- Erb, K.-H. et al. Unexpectedly large impact of forest management and grazing on global vegetation biomass. *Nature* **553**, 73–76 (2018).
- Paul, K. I. & Roxburgh, S. H. Predicting carbon sequestration of woody biomass following land restoration. *For. Ecol. Manage.* **460**, 117838 (2020).
- Anderson-Teixeira, K. J. et al. ForC: a global database of forest carbon stocks and fluxes. *Ecology* **99**, 1507 (2018).
- Powers, J. S., Corre, M. D., Twine, T. E. & Veldkamp, E. Geographic bias of field observations of soil carbon stocks with tropical land-use changes precludes spatial extrapolation. *Proc. Natl Acad. Sci. USA* **108**, 6318–6322 (2011).
- Stocker, T.F. et al. (eds) *Climate Change 2013: The Physical Science Basis. Contribution of Working Group I to the Fifth Assessment Report of the Intergovernmental Panel on Climate Change* (Cambridge Univ. Press, 2013).
- Zahawi, R. a., Holl, K. D., Cole, R. J. & Reid, J. L. Testing applied nucleation as a strategy to facilitate tropical forest recovery. *J. Appl. Ecol.* **50**, 88–96 (2013).
- Ashton, M. S. et al. Restoration of rain forest beneath pine plantations: a relay floristic model with special application to tropical South Asia. *For. Ecol. Manage.* **329**, 351–359 (2014).
- Teixeira, A. M. G., Soares-Filho, B. S., Freitas, S. R. & Metzger, J. P. Modeling landscape dynamics in an Atlantic rainforest region: implications for conservation. *For. Ecol. Manage.* **257**, 1219–1230 (2009).
- Sloan, S., Goosens, M. & Laurance, S. G. Tropical forest regeneration following land abandonment is driven by primary rainforest distribution in an old pastoral region. *Lands. Ecol.* **31**, 601–618 (2016).
- Chazdon, R. L. *Second Growth: The Promise of Tropical Forest Regeneration in an Age of Deforestation* (Univ. of Chicago Press, 2014).
- Speed, J. D. M., Martinsen, V., Mysterud, A., Holand, O. & Austrheim, G. Long-term increase in aboveground carbon stocks following exclusion of grazers and forest establishment in an alpine ecosystem. *Ecosystems* **17**, 1138–1150 (2014).
- Reid, J. L. et al. How long do restored ecosystems persist? *Ann. Missouri Botan. Gardens* **102**, 258–265 (2017).
- Paquette, A. & Messier, C. The role of plantations in managing the world's forests in the Anthropocene. *Front. Ecol. Environ.* **8**, 27–34 (2010).
- Smyth, C. E. et al. Quantifying the biophysical climate change mitigation potential of Canada's forest sector. *Biogeosciences* **11**, 3515–3529 (2014).

**Publisher's note** Springer Nature remains neutral with regard to jurisdictional claims in published maps and institutional affiliations.

© The Author(s), under exclusive licence to Springer Nature Limited 2020

## Methods

### Assembling a global carbon database

We systematically reviewed the literature (19 April 2017) with a Web of Science keyword search of studies published since 1975: TOPIC: (biomass OR carbon OR agb OR recover\* OR accumulat\*) AND (forest) AND (restorat\* OR reforest\* OR afforest\* OR plantation\* OR agroforest\* OR secondary\*). We included “agb” for aboveground biomass. We included “afforest\*” because afforestation sometimes describes establishing forest cover in places where forests historically occurred, but we eliminated studies that described tree planting in grasslands (also called ‘afforestation’), because these efforts are often not successful<sup>47</sup>, and reduce biodiversity and ecosystem integrity<sup>48,49</sup>.

The initial search yielded 10,937 peer-reviewed studies, which we augmented to 11,360 with additional peer-reviewed studies referenced therein or datasets from institutions (Oak Ridge National Laboratory, International Centre for Research in Agroforestry, and the Chinese Academy of Forestry). We reviewed all abstracts to identify accessible studies that described any approach for returning forest cover to the landscape (Extended Data Table 1). We fully reviewed these ( $N=5,464$ ) to find studies that quantified carbon or biomass stocks ( $N\approx 1,400$ ). We categorized the latter by approach for restoration of forest or tree cover and focused initially on natural forest regrowth ( $N=256$  studies) given the need for improved natural forest regrowth data and the immense time required to build this dataset. However, other approaches, such as assisted regeneration, are currently being reviewed for future studies.

To be included, studies had to provide: (1) empirical measures of carbon (or biomass) in aboveground or belowground plant, litter, coarse woody debris and/or soil pools; (2) stand age with at least one stand between 5 and 30 years old; and (3) a latitude and longitude, or a discernible geolocation (such as an identifiable place name). Papers focusing on soils did not need to include other carbon pools but had to include mineral soils deeper than 10 cm, as well as a reference measurement (for example, a younger stand or an adjacent non-forest plot) to assess changes in soil carbon. We included measurements in shallower soils if present in papers with data from soils 30 cm or deeper. Similarly, we extracted all available data from stands between 0 and 100 years old when included in studies with the correct age range (5 to 30 years old), excluding studies with only very young forests because of the stochastic nature of early forest establishment, as well as papers with only forests greater than 30 years old, given our 2020 to 2050 focus.

To avoid duplicated measurements, we gave priority to primary studies and included the earliest instance of repeatedly published data. Our dataset fully encompasses all relevant primary studies from many other reviews (for example, refs.<sup>19,27,36,50–56</sup>) and the Forest Carbon Database (ForC)<sup>35</sup>. For these, we obtained the original studies to confirm numbers, correct errors and acquire additional variables. However, we preferentially extracted data from three reviews rather than the primary source when authors acquired and reanalysed original datasets, some of which were previously unpublished<sup>57</sup> or were published in Russian or Chinese<sup>58,59</sup>. Notably, Guo and Ren<sup>58</sup> provided 5,730 measurements across China that we included in the larger dataset, but ultimately excluded by our more stringent filtering (details below).

Beyond geolocation, stand age (years), type of carbon pool, and carbon or biomass estimate ( $\text{Mg ha}^{-1}$ ), we also extracted any available data on type and intensity of previous land use or disturbance. We used geolocation to extract biome designations from refs.<sup>60,61</sup>. While we acquired data from presumably forested portions of tropical and temperate savannas (for example, the Miombo forests (mainly *Brachystegia* spp.) in Africa, the Cerrado savanna in Brazil, and the pinyon/juniper forests in the USA), we note that it is not ecologically appropriate to increase forest cover in many areas of savanna and that we do not advocate expansion of trees on natural, low-tree-cover landscapes<sup>48,49</sup>. We did not include mangroves because they are highly dynamic systems

that require complex accounting for in situ versus exported soil carbon accumulation<sup>62</sup>.

The resulting dataset includes 13,033 empirical measurements of carbon storage in aboveground and belowground biomass, soil, litter and coarse woody debris (see Supplementary Tables S3–S5). We aggregated data by site ( $N=2,330$ ) and plot ( $N=6,674$ ), where sites have unique geolocations and plots are spatial units within sites that have unique attributes (for example, age and previous land use; see metadata in Supplementary Information for additional details). We then further winnowed these data along stricter criteria to exclude (1) locations with inappropriate geolocations, such as in the ocean or a non-forest biome according to the biome spatial layer<sup>60,61</sup>, (2) stands less than one year old because they are not (yet) undergoing natural forest regrowth, (3) Mediterranean forests and temperate savanna because the sample size was too low ( $N<10$  for any single pool), (4) studies with only shallow soil measurements (30 cm or less) because carbon in topsoil is highly dynamic and can dramatically underestimate overall soil carbon<sup>63</sup>, and (5) Guo and Ren<sup>58</sup> data because it contained many old stands with little to no plant biomass that we could not explain. The final dataset ( $N=227$  studies) used in these analyses spanned 5,762 carbon measurements, 3,058 unique forest plots, 554 sites, 121 ecoregions and most forest and savanna biomes (Extended Data Fig. 7).

### Standardizing data across publications

For studies that reported biomass only, we converted to carbon ( $\text{Mg C ha}^{-1}$ ) using 0.47 as a default conversion factor for aboveground and belowground carbon pools (combined and described as the “total plant carbon” pool)<sup>64</sup>, 0.37 for litter biomass<sup>65</sup>, and 0.50 for coarse woody debris biomass<sup>66</sup>. If a study used different default conversion factors, we adjusted their carbon numbers to match the above defaults for consistency.

Most soil organic carbon (SOC) data (72%;  $N=1,065$  of 1,485) were already in units of  $\text{Mg C ha}^{-1}$  per centimetre depth and the remainder we converted from SOC concentration (g per 100 g) or soil organic matter (SOM). For SOM concentration data ( $N=38$ ), we estimated SOC concentration as SOM/2 based on ref.<sup>67</sup>, which found that the median ratio between SOM and SOC across 481 data points from 24 empirical studies was 1.97, with a mean of 2.20. We converted SOC concentration to  $\text{Mg C ha}^{-1}$  per centimetre depth with empirical bulk density data where given ( $N=355$ ) or depth-specific bulk density data from SoilGrids<sup>68</sup> ( $N=65$ ). SoilGrids provides bulk density modelled at 15 cm, 30 cm and 60 cm and we used the value nearest in depth to the SOC concentration measure. Modelled bulk density was higher but within the range of empirical estimates ( $1.29 \pm 0.13 \text{ Mg m}^{-3}$  versus  $0.98 \pm 0.31 \text{ Mg m}^{-3}$ , mean  $\pm$  standard deviation). To convert to  $\text{Mg C ha}^{-1}$  per centimetre depth, we used one bulk density value for each site and reference pairing, using measured bulk density from the pre-forest site if available, measured bulk density from the youngest nearby site as the next option, or SoilGrids bulk density from the pre-forest site in the absence of other data.

After converting biomass data to carbon, we standardized within pools. Aboveground carbon measures typically included foliage, but we retained two measures that excluded foliage, since this represents a small fraction of overall carbon. Studies differed in whether they included understory (such as lianas and shrubs). For those without, we added average understory carbon per biome based on our dataset (1.2  $\text{Mg C ha}^{-1}$  to 4.0  $\text{Mg C ha}^{-1}$ ). We did not, however, adjust for differences in diameters at breast height (DBH; nominally 1.3 m above ground level). Although studies used different DBH thresholds, ranging from 0 cm to 10 cm, minimum DBH did not explain variation in aboveground biomass ( $F_{1,459,2}=0.5, P=0.4608$ ) and we assumed that authors used a DBH threshold that captured the majority of biomass at their sites. We summed aboveground and belowground plant carbon using empirically measured belowground carbon when present ( $N=444$ ) or standard root-to-shoot ratios<sup>69</sup> when absent ( $N=2,346$ ). Where it was

# Article

possible to compare, we found that estimated belowground carbon was 1.8 Mg C ha<sup>-1</sup> higher than measured values, since the field measurements typically only quantified biomass to a specific depth or roots greater than a specific diameter. This produced 2,790 independent plot measurements of total plant carbon. For dead pools (litter and coarse woody debris), measurements often included additional pools, but we did not attempt to parse litter or coarse woody debris from these combined measurements because these pools are highly variable and site-specific<sup>65</sup>. Thus, we only retained single pool measurements ( $N=473$  litter and 298 coarse woody debris). Finally, for soil, we adjusted data to the nearest of two standard depths (30 cm and 60 cm). For plots with multiple depth measures, we used the slope from a fitted log–log curve for cumulative SOC stocks as a function of depth to estimate SOC at standard depths, but for plots without multiple depth measures, we used a biome-specific slope coefficient<sup>70</sup>. If standardizing depths resulted in duplicate measures—for example, when a study reported SOC at 20 cm and 40 cm, leading to two predicted values at 30 cm—we calculated the average. Depth-standardized SOC was 1% lower than the empirical measure of SOC and highly correlated ( $R^2=0.84$ ).

For plant, litter and coarse woody debris pools, we analysed carbon stocks (Mg C ha<sup>-1</sup>) as a function of stand age, as these pools can have zero carbon at initiation of regrowth. However, SOC changes are relative to a non-zero baseline so we first converted SOC stock data to rates (Mg C ha<sup>-1</sup> yr<sup>-1</sup>). For repeated measure designs, we calculated a single rate per plot based on SOC change from initial conditions. For the remaining studies, we used linear regression to fit SOC as a function of stand age within each chronosequence, treating any reference plot (for example, an adjacent treeless cropland) as age zero ( $N=5$  data points on average per regression). We only compared forest and reference plots with the same previous land use<sup>36</sup>. This produced a single rate estimate per chronosequence, and these rates became the foundational data for the soil analyses. We ultimately derived 138 SOC rates from chronosequences ( $N=129$ ) and repeated measures ( $N=9$ ). Most rates quantified changes at 0–30 cm ( $N=83$ ) and then 0–60 cm ( $N=55$ ).

## Potential drivers of carbon accumulation rates

To assess fundamental drivers of variation in carbon accumulation rates, we examined differences in rates (1) across biomes as a proxy for major climatic differences, (2) across soil texture categories (soil only), (3) as a function of type of previous disturbance or land use, and (4) as a function of intensity of previous disturbance or land use.

First, to examine differences in plant, litter, and coarse woody debris carbon among biomes, we used mixed effects models (R v. 3.5.1 packages lme4 and lmerTest) to examine carbon stocks as a function of stand age, biome and stand age  $\times$  biome with site (or plot nested within site) as a random intercept. We were primarily interested in the interaction term here and below, since it describes how the effect of age on carbon stocks (that is, carbon accumulation rate) is modified by the predictor variable, which in this case is biome. We compared a linear model to one with ln-transformed stand age, selecting the model that minimized the Aikake Information Criterion. For litter and coarse woody debris, carbon either declined nonlinearly from initial starting conditions or remained roughly constant with stand age (Extended Data Fig. 2). We therefore did not further examine carbon accumulation in these pools, because residual dead matter from previous disturbance obscured any signal of additional accumulation. However, we did examine variation across biomes by removing stand age from the model. We found that litter and coarse woody debris carbon stocks were generally higher in boreal and temperate biomes compared to other biomes (Extended Data Fig. 3; litter:  $F_{5,138.7}=8.5, P<0.0001$ ; coarse woody debris:  $F_{4,125.7}=5.9, P=0.0002$ ). For soil, we used linear regression to model carbon accumulation rates as a function of biome identity. We also included depth as a categorical predictor (depth and depth  $\times$  biome) and found that, although stocks generally declined with depth of measurement as expected, rates of carbon accumulation did not ( $F_{1,126}<0.1, P=0.956$ ).

Second, we examined how soil carbon accumulation might differ by soil texture. We used SoilGrids data on clay, silt and sand percentages to estimate the soil texture category (for example, sand, loam, clay and so on) at each site where texture data were not provided. We used linear regression to analyse soil carbon accumulation as a function of texture, and again found that texture was not a significant predictor of variation ( $F_{9,128}=0.2, P=0.9997$ ).

Third, we examined how previous land use or disturbance influenced carbon stocks over time for disturbance types with more than three data points per biome. When studies listed multiple disturbance or land use types for a single plot, we noted the most recent type where discernible. Otherwise, we used the type that was most likely to negatively affect forest regrowth (natural disturbance < harvest = shifting cultivation < crop < pasture, based on personal observations). We conducted separate analyses per biome, as each biome was associated with different disturbance types. For plant biomass ( $N=2,600$ ), we used mixed effects linear regression, modelling carbon as a function of stand age and previous land use, plus their interaction, with site (or plot nested within site) as a random intercept. For soil ( $N=132$ ), we used an analysis of variance with previous land use and depth as the predictors of SOC.

Finally, we examined how the intensity of previous disturbance influences carbon stocks over time. Unfortunately, studies provided fewer details about the intensity of previous land use ( $N=1,567$  and 91 for plant biomass and SOC respectively). Three authors in this study (H.P.G., K.D.H. and C.L.) independently categorized disturbance intensity into low, medium and high categories using a disturbance rubric (see Supplementary Table S1), assigning the final category based on majority agreement among scorers. Given data scarcity, we only categorized intensity of previous land use for four disturbance types: pasture, shifting cultivation, long-term cropland, and clear-cut harvest. We conducted our statistical analysis across disturbance types, using mixed effects to model total plant carbon as a function of stand age and disturbance intensity, plus their interaction, with site or plot nested within site and biome as random intercepts. We used a similar model for soil with only disturbance intensity as the predictor and biome as a random intercept. We also ran similar models, though without the biome random effect, for each biome with sufficient data.

## Mapping global, near-term forest carbon accumulation potential

To develop maps of aboveground carbon accumulation, we extracted the literature-derived data that had a separate measurement for aboveground carbon and stand age of 30 years or less ( $N=2,118$ ). We next improved the geographic and environmental representativeness of our aboveground dataset by including available national forest inventory data from three countries: Australia, Sweden and the USA (Extended Data Fig. 7). The Australian data were collected between 2006 and 2017 from naturally regenerating stands of known age ( $N=54$ )<sup>34</sup>. These stands were located across contrasting biomes, ranging from relatively productive temperate regions to water-stressed semi-arid regions. Biomass data included only new tree growth and did not include remnant trees. The Swedish National Forest Inventory plot data were collected between 2007 and 2017 ( $N=5,458$ )<sup>71</sup>. The USA data are from the United States Department of Agriculture (USDA) Forest Service's Forest Inventory and Assessment (FIA) programme ( $N=5,482$ )<sup>34</sup>. Owing to privacy concerns, FIA data are made available only after a fraction of plots are randomly shifted or swapped with the coordinates of others in the same county. Although these security procedures shifted the geolocation of plot data and predictor variables by approximately 1 km, including the FIA data improved the predictive power of the model. We used plots that had (1) been remeasured at time one ( $T_1$ ) and time two ( $T_2$ ) to estimate a rate of carbon accumulation, (2) no treatment at  $T_2$  or  $T_1$  (TRTCD=0) to restrict data to natural forest regrowth, (3) no trees recorded as alive in  $T_2$  that were recorded as dead in  $T_1$  (DEAD\_TO\_LIVE\_COUNT=0) to remove erroneous measurements, (4) no recorded disturbance in  $T_2$  or

$T_1$  (DSTRBCD = 0), (5) aboveground biomass at  $T_2$  (AG\_LIVE\_BIO\_MGHA > 0) to avoid harvested or burned plots, and (6) a stand age at  $T_2$  between 0 and 30 years ( $30 > \text{STDAGE} > 0$ ). We also only included plots where >50% of the area was comprised of the same forest type, owner class, land class and other properties at  $T_1$  and  $T_2$  to ensure consistency within a site (CONDPROP\_UNADJ > 0.5).

Combined, all literature-derived and national inventory data represented 13,112 plot measurements. We then calculated carbon accumulation rates by dividing aboveground carbon by stand age, providing an average rate over the first 30 years of growth. We removed plots that did not fall into forest or savanna biomes or had no recorded biomass to avoid plots that had probably been harvested ( $N = 685$  or 5.2% of data). We also removed any points that had rates greater than three standard deviations above the mean ( $N = 153$  or 1.2% of data). Finally, when there were multiple point estimates within each of our ~1-km pixels, we calculated the average rate to use in model development ( $N = 10,216$ ). Averaging within pixels improved model performance compared to models with no within-pixel averaging.

To create a spatially predictive model of carbon accumulation, we first sampled our prepared stack of 66 environmental covariates at each of the point locations within the literature-derived and national inventory datasets. These layers included climate, soil nutrient, soil chemical, soil physical, radiation, topography and nitrogen deposition variables (see Supplementary Table S2). We did not use variables that represent current vegetation condition (for example, leaf area index or percent forest cover) or satellite-derived indices such as the normalized difference vegetation index (NDVI), as these do not represent fundamental biophysical controls on carbon accumulation rates for the future accumulation of plant biomass. We re-sampled and re-projected these covariate map layers to a unified pixel grid (World Geodetic System 1984, EPSG:4326) at 30-arcsecond resolution (~1-km at the Equator), downsampling higher resolution data using the mean aggregation method and resampling those with a lower original resolution using simple upsampling (that is, without interpolation). We chose this resolution to balance pixel-level uncertainty, which is proportionately larger in smaller pixels, with utility for local decision-makers. If multiple resolutions were available for a covariate, we used the resolution closest to 30 arcseconds. Covariates represent different time periods but were all between 1970 and 2017. This time period allows us to capture long-term average conditions under current and historical climate.

We then split the total number of points into a training set and a test set using an 80/20 random split, stratified by data source (that is, the literature-derived data and each national inventory) and by biome. We used the training set to determine the best machine-learning algorithm and set of hyperparameters, and to train the final model. We used the test set to assess out-of-sample error, as well as model performance with novel data (details below).

We compared four machine-learning algorithms (random forest<sup>72</sup>, a gradient boosting decision tree called XGBoost<sup>73</sup>, support vector machines<sup>74</sup>, and multi-layer perceptron)<sup>75</sup> along with four feature selection methods (support vector machine feature selection, random-forest-based feature selection, principal component analysis, and no feature selection), leading to 16 different combinations of feature selection methods and machine-learning algorithms (or ‘model pipelines’). Each model pipeline first applied feature scaling to the data (standard scaling for the continuous variables and one-hot encoding of biome as our only categorical variable), then selected features using the feature selection algorithm, and finally trained the machine-learning model on the transformed data. For each machine-learning algorithm, we also defined a suite of hyperparameters to test over, often leading to over 1,000 tested hyperparameter combinations. We conducted the machine learning steps in Microsoft Azure.

We used the Python scikit-learn package and the gridsearchCV function to define and train model pipelines using three-fold cross-validation and to choose the best hyperparameter combination

for each model pipeline<sup>76</sup>. We used the cross-validation RMSE to choose the best feature selection method and machine-learning algorithm with defined hyperparameters. Cross-validation is an important step in training and comparing machine-learning algorithms, as it creates pseudo-training sets that can be used to estimate the out-of-sample error and reduce over-fitting to the training set, while still keeping the final test set completely independent of the model. In three-fold cross-validation, the training set is randomly split into three equal-sized subsets. Two subsets combine to form a new training subset, and the last subset serves as a validation set to assess the model performance. We trained the model pipeline on the training subset, stored the RMSE of the model predictions over the validation set, and then repeated the process twice more with the remaining combinations of training and validation subsets. The final cross-validation score is the average of the validation RMSEs across each model pipeline, and we used the average cross-validation RMSE to compare model pipelines and selected the model pipeline with the lowest cross-validation RMSE as our best trained model pipeline. In our case, the best trained model pipeline was the random forest machine-learning algorithm with no feature selection.

After determining the best-performing algorithm and set of hyperparameters, we used a Monte Carlo approach to create an ensemble model for our final predictions and uncertainty analysis. We generated the ensemble model by first drawing 100 independent bootstrapped samples with replacement of our training data, stratified on the data source and biome. Next, we trained separate random forest models using the best-performing set of hyperparameters on each of the 100 bootstrapped samples of the training data. Our final model is the ensemble of the 100 random forest models, where the ensemble model prediction is the average of the predictions of the 100 random forest models. To assess our out-of-sample error, we applied this final ensemble model to our test set. The ensemble model had an RMSE of 0.798 Mg C ha<sup>-1</sup> yr<sup>-1</sup> and an  $R^2$  of 0.445 on our independent test set.

To create a final global map of aboveground carbon accumulation and associated uncertainty, we sampled all environmental covariate layers over all pixels in forest and savanna biomes and applied the best trained model to each pixel’s covariates. Although the trained model works over any area, we constrained it to forest and savanna biomes. Because our model is an ensemble of 100 random forest models with each random forest model trained on an independent bootstrapped sample of the training data, we can use the standard deviation of the 100 random forest models’ predictions to estimate model uncertainty in each pixel. Therefore, for each pixel we have the model’s prediction and standard deviation across the 100 models.

We also tested the extent of extrapolation in our models by examining how many of the Earth’s pixels exist outside the range of our sampled data for each of the 66 global covariate layers. We first extracted the minimum and maximum values of each covariate layer across our sampling pixels to determine sample range. We then used the final model to evaluate the number of variables that fell outside the sample range, across all terrestrial pixels. Next, we created a per-pixel representation of the relative proportion of interpolation and extrapolation (Extended Data Fig. 5). This revealed that our samples covered most environmental conditions on Earth, with 88% of Earth’s pixel values falling within the sampled range of at least 90% of all bands. Across all pixels, the average fraction of the pixel values falling within the sampled range of the covariates was 97%. This method measures the univariate extent of extrapolation, and takes into account only whether each of the pixel’s covariates falls into the sampled range of the corresponding covariate from our training points.

#### Comparison of rates to IPCC defaults

We compared our predicted rates with the latest 2019 IPCC default rates for young forest (less than 20 years old)<sup>5</sup> by estimating the

# Article

average pixel value, as well as the minimum and maximum pixel value within each ecozone by continent combination. Although the IPCC provides default rates for the first 20, rather than the first 30, years of forest regrowth described here, we modelled linear rates, assuming growth rates would not be asymptotic until later in stand development. Therefore, because our map would not change using a 20-year time horizon, our results are directly comparable to IPCC default rates. Whenever a range was provided for IPCC values, we used the average of the lower and upper bound of the range to compare to our predicted rates.

## Climate mitigation potential of natural forest regrowth

To estimate the ‘maximum’ mitigation potential of natural forest regrowth (constrained by biodiversity and human well-being considerations), we combined the Griscom et al.<sup>3</sup> area map with our map of potential aboveground carbon accumulation and a map of potential belowground plant carbon accumulation. We created the latter by applying default root-to-shoot ratios to the aboveground pixels<sup>5</sup>. This Griscom et al.<sup>3</sup> extent raster identifies more area of opportunity than is available because there is a series of non-spatial deductions that was applied later in their analyses. We therefore proportionally scaled mitigation opportunity within each country so that the final area summed to their reported 678 Mha area of opportunity. The Griscom et al.<sup>3</sup> analysis assumes that a small fraction of their area of opportunity would have plantations, so we adjusted their mitigation estimate to reflect a scenario of 100% natural forest regrowth (2.88 Pg C yr<sup>-1</sup>).

Lewis et al.<sup>12</sup> compiled national commitments to the Bonn Challenge and from nationally determined contributions to the Paris Agreement. Although that publication focused on tropical countries, we acquired the global compilation to use here. Two countries (Niger and Burkina Faso) included commitments that we did not include, because those countries fall outside our potential rates map. To estimate the mitigation potential of these national commitments, we used the same average predicted rates per country from the overlay of Griscom et al.<sup>3</sup> for aboveground and belowground carbon accumulation. Thus, this assumes that the 349 Mha of opportunity under this scenario represents an average subset of the area identified as biophysically possible in Griscom et al.<sup>3</sup>.

## Data availability

The literature-based dataset (both raw and filtered) and detailed descriptions of the environmental covariates are all available at <https://github.com/forc-db/groa>, where GROA stands for Global Restoration Opportunity Assessment. Data are also archived on Zenodo at <https://doi.org/10.5281/zenodo.3983644>. The Supplementary Information includes metadata for the literature-derived dataset (Supplementary Table S3, Supplementary sections 4 and 5). We also include data on country-level estimates (see Supplementary Data 1). Spatial data for both aboveground carbon accumulation rates and uncertainty (scaled and unscaled by mean pixel value), as well as belowground carbon accumulation rates can be downloaded from Global Forest Watch (<http://www.globalforestwatch.org>). S.C.C.-P. and N.H. welcome discussions around potential collaborations, and the data are freely available. Source data are provided with this paper.

## Code availability

We include code for constructing the global maps and assessing uncertainty at <https://github.com/forc-db/groa>.

47. Cao, S. Why large-scale afforestation efforts in China have failed to solve the desertification problem. *Environ. Sci. Technol.* **42**, 8165 (2008).
48. Veldman, J. W. et al. Where tree planting and forest expansion are bad for biodiversity and ecosystem services. *Bioscience* **65**, 1011–1018 (2015).
49. Bond, W. J. Ancient grasslands at risk. *Science* **351**, 120–122 (2016).

50. Crouzeilles, R., Ferreira, M. S. & Curran, M. Forest restoration: a global dataset for biodiversity and vegetation structure. *Ecology* **97**, 2167 (2016).
51. Deng, L., Shangguan, Z. P. & Sweeney, S. ‘Grain for Green’ driven land use change and carbon sequestration on the Loess Plateau, China. *Sci. Rep.* **4**, 7039 (2015).
52. Bárcena, T. G. et al. Soil carbon stock change following afforestation in Northern Europe: a meta-analysis. *Glob. Change Biol.* **20**, 2393–2405 (2014).
53. Marín-Spiotta, E. & Sharma, S. Carbon storage in successional and plantation forest soils: a tropical analysis. *Glob. Ecol. Biogeogr.* **22**, 105–117 (2013).
54. Deng, L., Zhu, G., Tang, Z. & Shangguan, Z. Global patterns of the effects of land-use changes on soil carbon stocks. *Glob. Ecol. Conserv.* **5**, 127–138 (2016).
55. Zhang, K., Dang, H., Zhang, Q. & Cheng, X. Soil carbon dynamics following land-use change varied with temperature and precipitation gradients: evidence from stable isotopes. *Glob. Change Biol.* **21**, 2762–2772 (2015).
56. Becknell, J. M., Kissing, L. & Powers, J. S. Aboveground biomass in mature and secondary seasonally dry tropical forests: a literature review and global synthesis. *For. Ecol. Manage.* **276**, 88–95 (2012).
57. Poorter, L. et al. Biomass resilience of Neotropical secondary forests. *Nature* **530**, 1–15 (2016).
58. Guo, Q. & Ren, H. Productivity as related to diversity and age in planted versus natural forests. *Glob. Ecol. Biogeogr.* **23**, 1461–1471 (2014).
59. Krainka, O. *NPP Boreal Forests: Siberian Scots Pine Forests, Russia, 1968–1974, R1* <http://daac.ornl.gov> (Oak Ridge National Laboratory, 1995).
60. Dinerstein, E. et al. An ecoregion-based approach to protecting half the terrestrial realm. *Bioscience* **67**, 534–545 (2017).
61. Olson, D. M. et al. Terrestrial ecoregions of the world: a new map of life on Earth. *Bioscience* **51**, 933–938 (2001).
62. Chew, S. T. & Gallagher, J. B. Accounting for black carbon lowers estimates of blue carbon storage services. *Sci. Rep.* **8**, 2553 (2018).
63. James, J., Devine, W., Harrison, R. & Terry, T. Deep soil carbon: quantification and modeling in subsurface layers. *Soil Sci. Soc. Am. J.* **78**, S1–S10 (2014).
64. Aalde, H. et al. Forest land. In *2006 IPCC Guidelines for National Greenhouse Gas Inventories. Volume 4: Agriculture, Forestry and Other Land Use* (eds Paustian, K. et al.) Ch. 4 (IPCC, 2006).
65. Aalde, H. et al. Generic methodologies applicable to multiple land-use categories. In *2006 IPCC Guidelines for National Greenhouse Gas Inventories. Volume 4: Agriculture, Forestry and Other Land Use* (eds Paustian, K. et al.) Ch. 2 (IPCC, 2006).
66. Russell, M. B. et al. Quantifying carbon stores and decomposition in dead wood: a review. *For. Ecol. Manage.* **350**, 107–128 (2015).
67. Pribyl, D. W. A critical review of the conventional SOC to SOM conversion factor. *Geoderma* **156**, 75–83 (2010).
68. Hengl, T. et al. SoilGrids250m: global gridded soil information based on machine learning. *PLoS One* **12**, e0169748 (2017).
69. Mokany, K., Raison, R. J. & Prokushkin, A. S. Critical analysis of root:shoot ratios in terrestrial biomes. *Glob. Change Biol.* **12**, 84–96 (2006).
70. Jobbágy, E. G. & Jackson, R. B. The vertical distribution of soil organic carbon and its relation to climate and vegetation. *Ecol. Appl.* **10**, 423–436 (2000).
71. Swedish National Forest Inventory Sample Plot Data <https://www.slu.se/en/Collaborative-Centres-and-Projects/the-swedish-national-forest-inventory/listor/sample-plot-data/> (SNFI, 2019).
72. Breiman, L. Random forests. *Mach. Learn.* **45**, 5–32 (2001).
73. Chen, T. & Guestrin, C. XGBoost: a scalable tree boosting system. In Proc. 22nd ACM SIGKDD Int. Conf. on Knowledge Discovery and Data Mining 785–794 (Association for Computing Machinery, 2016).
74. Cortes, C. & Vapnik, V. Support-vector networks. *Mach. Learn.* **20**, 273–297 (1995).
75. Rosenblatt, F. The perceptron: a probabilistic model for information storage and organization in the brain. *Psychol. Rev.* **65**, 386–408 (1958).
76. Pedregosa, F., Varoquaux, G., Gramfort, A., Michel, V. & Thirion, B. Scikit-learn: machine learning in Python. *J. Mach. Learn. Res.* **12**, 2825–2830 (2011).
77. Chazdon, R. L. et al. Carbon sequestration potential of second-growth forest regeneration in the Latin American tropics. *Sci. Adv.* **2**, e1501639 (2016).
78. Shono, K., Cadaweng, E. A. & Durst, P. B. Application of assisted natural regeneration to restore degraded tropical forestlands. *Restor. Ecol.* **15**, 620–626 (2007).
79. Nieuwenhuis, M. Terminology of forest management. In *International Union of Forest Research Organizations World Series Vol. 9-en* (IUFRD, 2000).
80. Winrock International AFOLU Carbon Calculator. *The Agroforestry Tool: Underlying Data and Methods* (USAID and Winrock International, 2014).
81. Vieira, D. L. M., Holl, K. D. & Peneireiro, F. M. Agro-successional restoration as a strategy to facilitate tropical forest recovery. *Restor. Ecol.* **17**, 451–459 (2009).

**Acknowledgements** We thank the Children’s Investment Fund Foundation, COnON Foundation, the Craig and Susan McCaw Foundation, the Doris Duke Charitable Foundation, the Good Energies Foundation, and Microsoft’s AI for Earth program for financial support. This paper was also developed with funding from the Government of Norway, although it does not necessarily reflect their views or opinions. We thank J. Adams, E. Brolis, A. Hector, J. Ghazoul, M. Hamsik, S. Lewis, B. Lurasci, R. Thadani, B. Tsang and A. Yang for the initial idea development at an Oxford University workshop in 2017. We thank G. Domke and B. Walters (USDA Forest Service) for providing fuzzed FIA plot data, J. Fridman (Swedish National Forest Inventory) for providing Swedish data, and H. Xu for providing raw biomass data from Jainfengling Nature Reserve (Hainan Island, China).

**Author contributions** S.C.C.-P., B.W.G., N.L.H., D.G., K.L., S.S. and L.X. designed the study with input from all authors. S.C.C.-P. contributed to and led all other facets of the study. S.M.L., K.J.A.-T., R.D.B., P.W.E., H.P.G., K.D.H., C.L., R.L., K.P., S.R., S.A.W., C.E.W., W.S.W. and B.W.G. contributed to database compilation, analyses and manuscript preparation. N.L.H., K.L., D.G., T.W.C., D.R., S.S., L.X. and J.v.d.H. constructed the global maps and contributed to manuscript preparation. G.L., R.L., V.H., K.P. and S.R. contributed to database compilation and manuscript

preparation. R.L.C., R.A.H., Y.M., P.M., A.P. and J.D.P. contributed to manuscript preparation. S.C.C.-P. is the corresponding author, handling requests for reprints and materials not included in the data repository.

**Competing interests** The authors declare no competing interests.

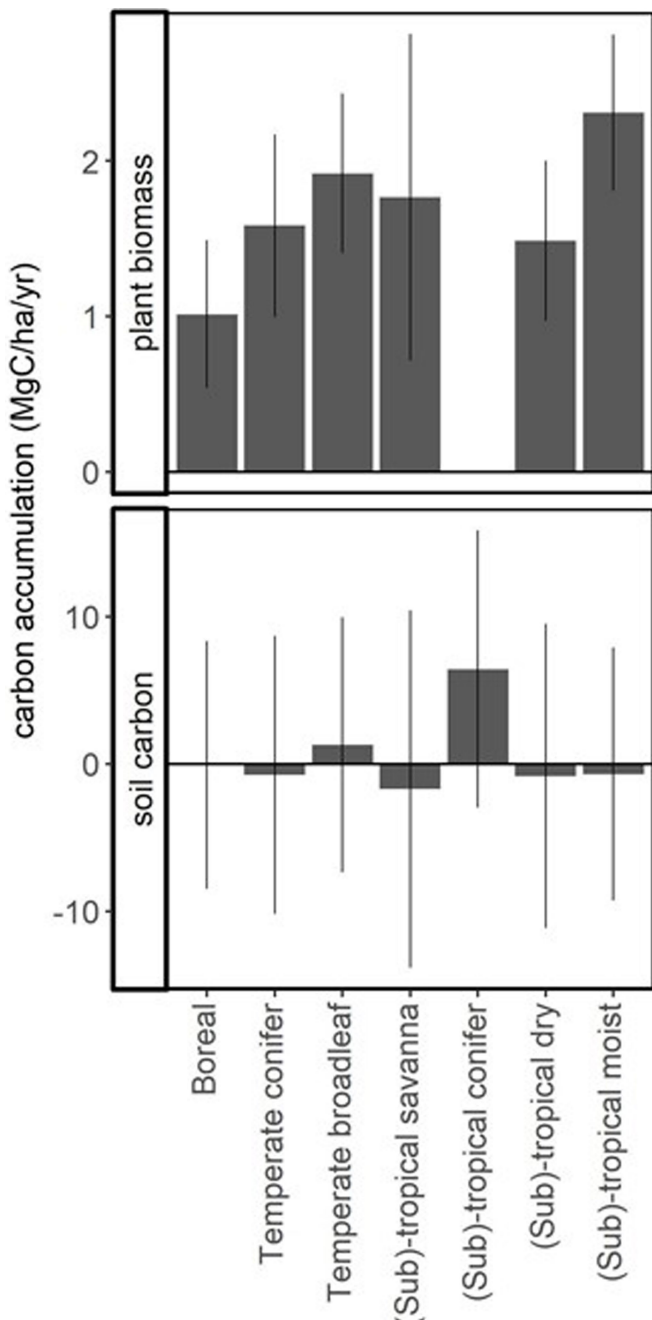
**Additional information**

**Supplementary information** is available for this paper at <https://doi.org/10.1038/s41586-020-2686-x>.

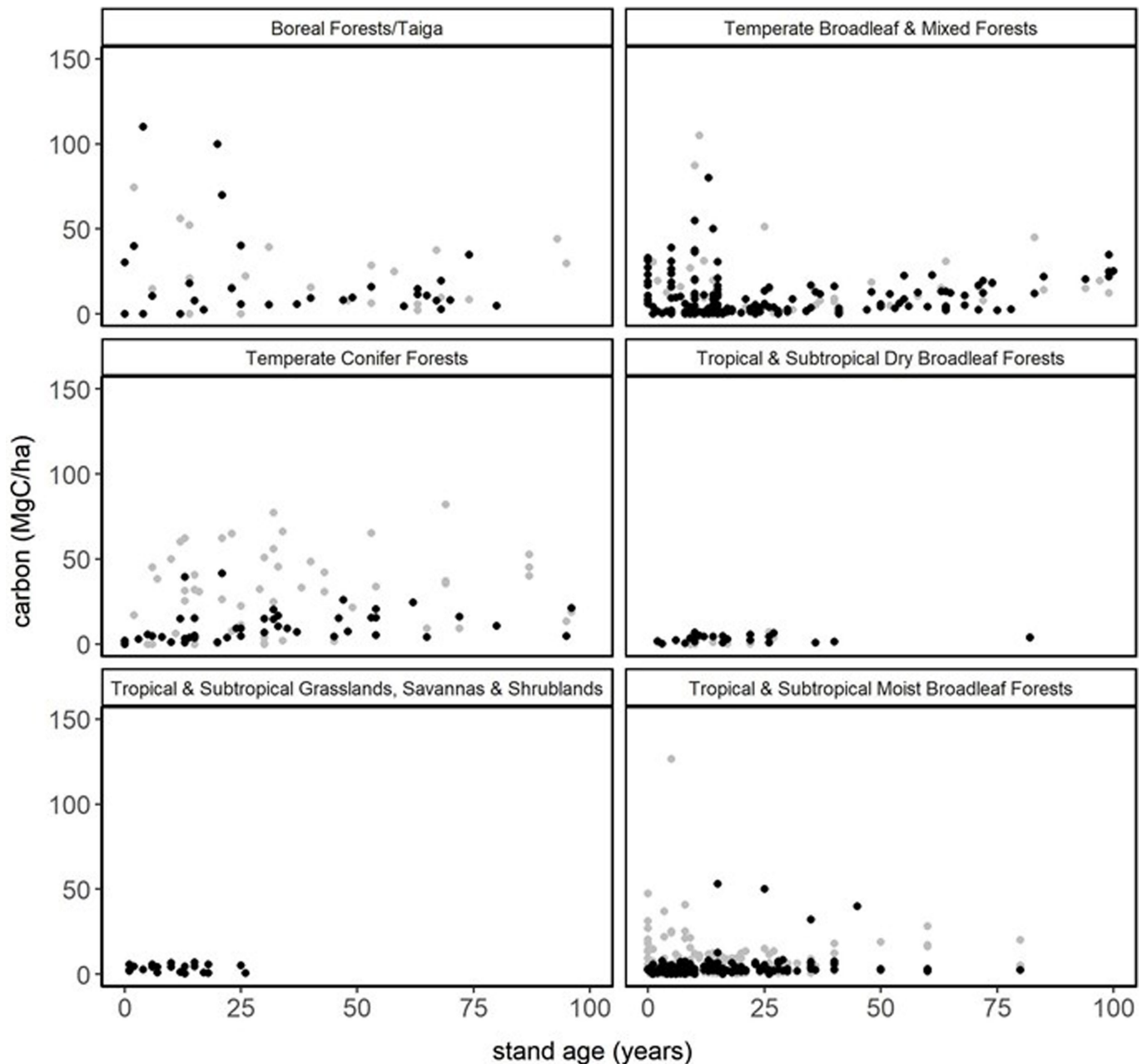
**Correspondence and requests for materials** should be addressed to S.C.C.-P.

**Peer review information** *Nature* thanks Michael Ryan, Edzo Veldkamp and the other, anonymous, reviewer(s) for their contribution to the peer review of this work.

**Reprints and permissions information** is available at <http://www.nature.com/reprints>.

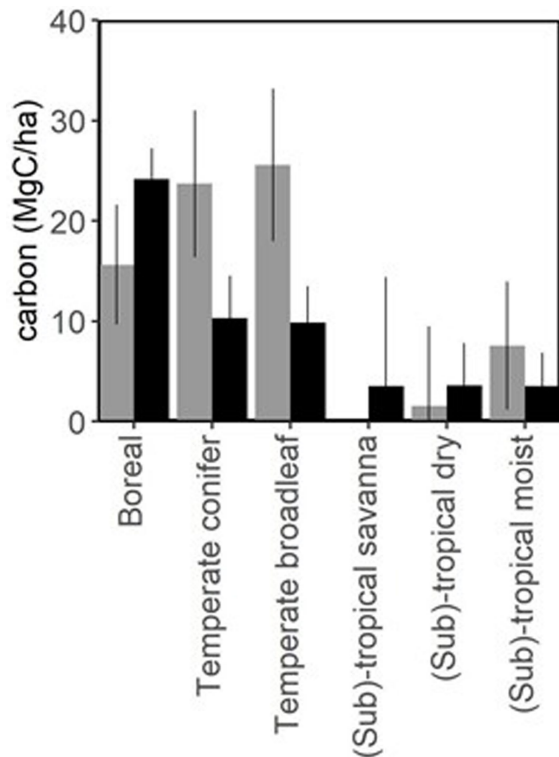
**Extended Data Fig. 1 | Variation in carbon accumulation among biomes.**

Observed variation in total plant carbon accumulation rates and soil carbon accumulation rates (mean  $\pm$  95% confidence intervals) from the literature-derived dataset. We did not have plant biomass data for subtropical and tropical conifer forests.

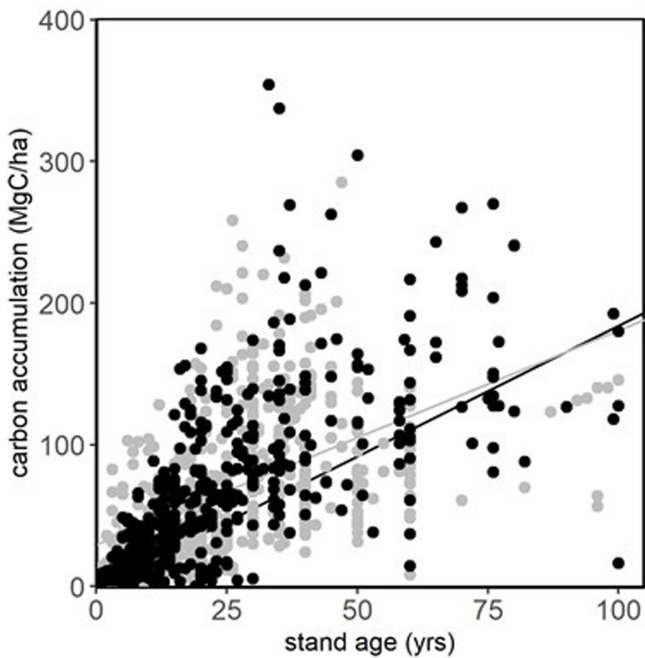


**Extended Data Fig. 2 | Accumulation of coarse woody debris and litter carbon through time.** We did not find studies describing litter (black) or coarse woody debris (grey) pools in temperate savannas, or coarse woody debris in tropical savannas.

## Article

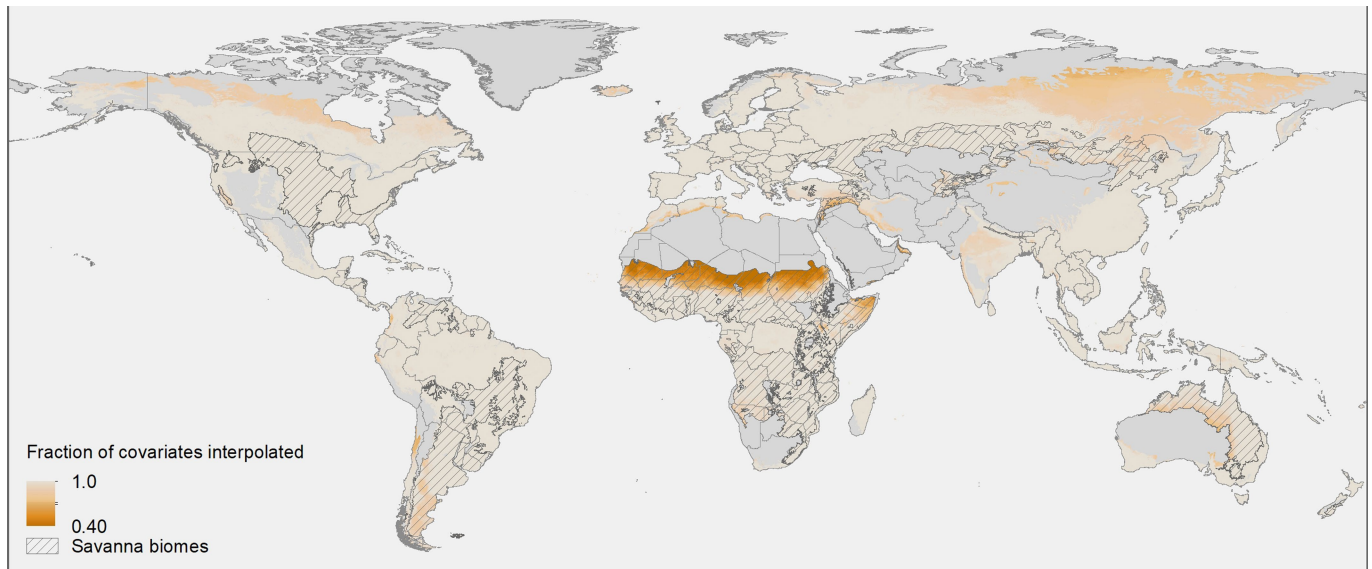


**Extended Data Fig. 3 | Variation in carbon stocks among biomes.** Carbon pools (mean  $\pm$  standard error) in coarse woody debris (grey) and litter (black).

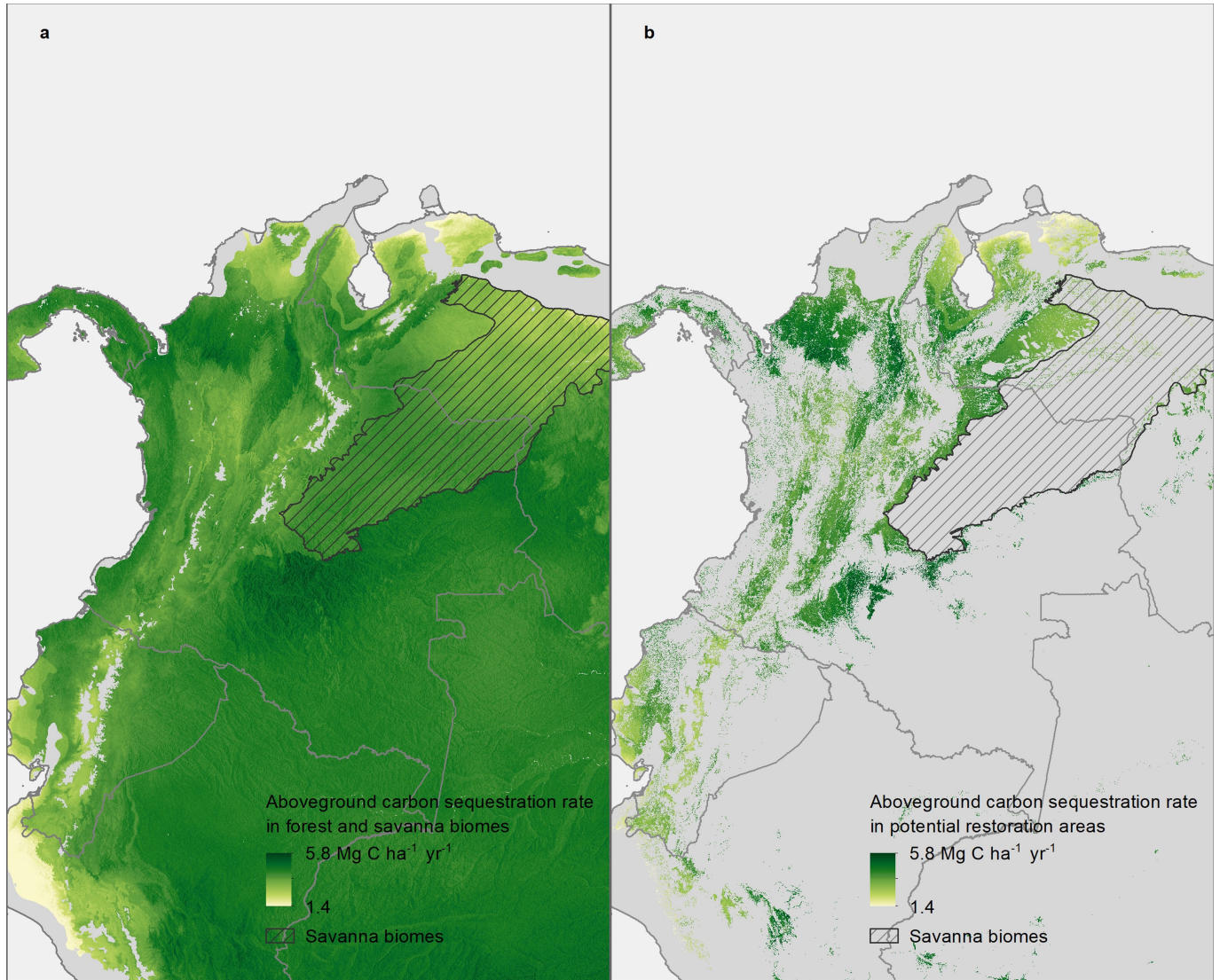


**Extended Data Fig. 4 | Effect of disturbance intensity on carbon accumulation.** Carbon accumulation in plots with high intensity disturbance (black circles, black line) versus low intensity disturbance (grey circles, grey line). The most disturbed categories had lower residual biomass at the initiation of regrowth (for example, 0  $\text{Mg C ha}^{-1}$  versus 28  $\text{Mg C ha}^{-1}$  in the least disturbed category; Welch's  $t$ -value = 5.9,  $P < 0.0001$ ), suggesting that the higher rate in the most disturbed category is due to standard sigmoidal growth rates in forests.

# Article

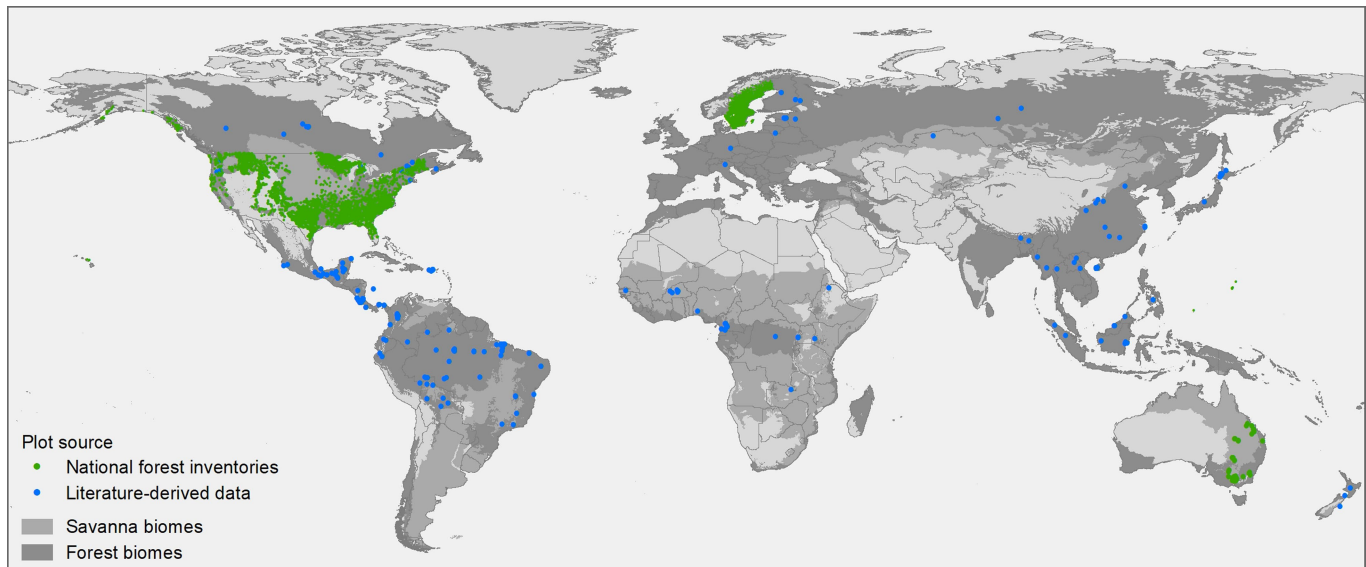


**Extended Data Fig. 5 | Map of extent of extrapolation per pixel across all covariate layers.** A value of 1 indicates that 100% of pixels fall within the sample range (that is, there is no extrapolation).



**Extended Data Fig. 6 | Fine-scale variation in rates.** **a**, Map of predicted carbon accumulation rates in Colombia, as an example. **b**, Map of predicted rates filtered to the area of opportunity in Griscom et al.<sup>3</sup> to demonstrate where these rates might apply.

# Article



**Extended Data Fig. 7 | Coverage of field data.** Distribution of sites after final filtering of the literature-based dataset (blue) and inclusion of the field inventory data (green). We compiled data from forest (dark grey) and savanna biomes (light grey). We restricted savanna data to portions of these grassland-forest matrices with forest cover >25%.

**Extended Data Table 1 | General approaches for restoring forest or tree cover**

Land-use	Type with Definitions
Semi-natural forest, protected or with some selective logging	<p><b>Natural forest regrowth</b> involves allowing forests to spontaneously regrow without any silvicultural interventions, though may involve removing disturbance factors (e.g., fire breaks, fencing, control of feral animals such as camels and goats, reduced grazing pressure)<sup>77</sup>. This includes both succession after abandonment and forest recovery following logging, fire or disturbances.</p> <p><b>Assisted natural regeneration</b> aims to accelerate natural forest regrowth and/or guide successional trajectories through activities that enhance tree growth, such as removing invasive grasses, liana cutting, and/or other practices<sup>78</sup>. We also include enrichment planting in this category.</p> <p><b>Active restoration</b> includes smaller tree configurations (e.g., applied nucleation methods), as well as large scale tree planting endeavors to restore native forests. Species may be mixed at the stand scale or in patches at the landscape scale. This strategy may also involve extensive natural forest regrowth following initial planting.</p>
Timber plantations	<p><b>Mixed species plantations</b> include at least two species intermixed on large areas in timber stands and may involve a mix of native and non-native species.</p> <p><b>Monoculture plantations</b> include plantation forests where the same species is grown on large areas in even-aged stands<sup>79</sup>. We include estimates for individual species that are commonly employed, as well as a more general estimate for species that are more infrequent. This includes both native and non-native species.</p>
Agroforestry	<p><b>Intensive tree monocrops</b> include all non-timber monocultures, such as fruit or nut tree monocultures, oil palm plantations, and other commodity crops.</p> <p><b>Multistrata systems</b> are those with a mix of under- and overstory species, and include home gardens and shade-grown cropping systems like cacao (<i>Theobroma cacao</i> L.) and coffee (<i>Coffea</i> sp.) combined with shade-, timber- or commercial tree crops<sup>81</sup>.</p> <p><b>Tree intercropping</b> includes agricultural systems where woody species are grown in crop fields, in scattered or systematic arrangements. These species may be used for fruit, fodder, fuelwood or timber<sup>80</sup>.</p> <p><b>Silvopastoral systems</b> include grazing under scattered or planted trees, as well as tree-fodder systems<sup>80</sup>.</p>
Transitional land use	The <b>transitional land use</b> strategy involves incorporating a range of agroforestry and/or plantation approaches in early stages of reforestation, as a transitional phase towards native forest restoration, to overcome socioeconomic and ecological obstacles to restoring these lands <sup>81</sup> .

This list is based on an aggregation of existing taxonomies and expert consultation at a workshop at Oxford University, UK, in February 2017. These approaches will not necessarily reach >25% forest cover. Categories are based on refs. <sup>77-81</sup>.

# Article

**Extended Data Table 2 | Effect of disturbance intensity on carbon accumulation**

biome	intensity	best fit (parameters ± standard error)	F-statistic (age × intensity), p-value	N
temperate broadleaf	L	(1.6 ± 0.2) × (age) + (-8.6 ± 28.8)	$F_{2,62.0} = 1.4, p = 0.248$	21
	M	(0.9 ± 0.7) × (age) + (12.7 ± 49.1)		5
	H	(1.2 ± 0.2) × (age) + (17.1 ± 14.6)		63
temperate conifer	L	(-58.5 ± 22.8) × ln(age) + (206.9 ± 63.9)	$F_{1,3.3} = 15.0, p = 0.024$	3
	H	(29.9 ± 5.5) × ln(age) + (-36.8 ± 20.8)		6
(sub)-tropical dry	L	(28.1 ± 4.3) × ln(age) + (-42.6 ± 19.3)	$F_{2,71.1} = 37.7, p < 0.0001$	292
	M	(17.0 ± 7.0) × ln(age) + (-18.3 ± 24.8)		22
	H	(62.8 ± 3.6) × ln(age) + (-124.2 ± 12.4)		126
(sub)-tropical moist	L	(2.5 ± 0.2) × (age) + (35.8 ± 6.1)	$F_{2,746.7} = 10.3, p < 0.0001$	282
	M	(2.6 ± 0.2) × (age) + (19.3 ± 1.9)		443
	H	(1.9 ± 0.1) × (age) + (23.3 ± 3.6)		255
(sub)-tropical savanna	L	(1.4 ± 0.3) × (age) + (-0.1 ± 9.9)	$F_{1,39.2} = 7.1, p = 0.010$	36
	H	(0.4 ± 0.3) × (age) + (3.0 ± 9.2)		12

Biome-level effects of disturbance intensity on carbon accumulation in total plant biomass ( $\text{Mg C ha}^{-1} \text{yr}^{-1}$ ) as a function of stand age. Intensity categories are low (L), medium (M), and high (H) based on Supplementary Table S1 and we list number of data points per category (N). For all biomes, the greatest carbon accumulation rate (slope parameter) was observed in the intensity category with the lowest starting biomass (intercept parameter).